JACS
JOURNAL OF THE AMERICAN CHEMICAL SOCIETY
Article
pubs.acs.org/JACS

Iterative Synthesis of Oligo[*n*]rotaxanes in Excellent Yield

James E. M. Lewis,[†,§] Joby Winn,[‡,§] Luca Cera,[‡] and Stephen M. Goldup*[,†]

[†]Chemistry, University of Southampton, Highfield, Southampton SO17 1BJ, U.K.
[‡]School of Biological Sciences, Queen Mary University of London, London E1 4NS, U.K.

Supporting Information

ABSTRACT: We present an operationally simple iterative coupling strategy for the synthesis of oligomeric homo- and hetero[*n*]rotaxanes with precise control over the position of each macrocycle. The exceptional yield of the AT-CuAAC reaction, combined with optimized conditions that allow the rapid synthesis of the target oligomers, opens the door to the study of precision-engineered oligomeric interlocked molecules.

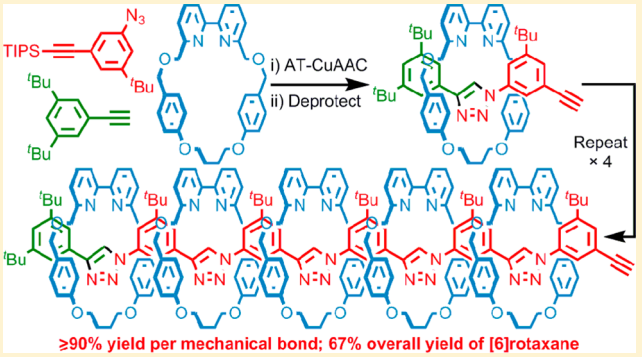

INTRODUCTION

Main-chain[1] oligo- and poly[*n*]rotaxanes typically consist of a linear axle component encircled by $(n - 1)$ macrocycles[2] that are prevented from escaping by bulky end groups.[3−6] The threaded arrangement of axle and rings gives rise to products with physical and chemical properties that are distinct from those of either component. As a result, poly[*n*]rotaxanes have been investigated for applications including drug delivery,[7] electronic materials,[8] stimuli-responsive materials,[9] and sensors,[10] and the mechanical properties of so-called "slide ring gels"[11] have led to their commercial application in scratch-resistant surfaces.

The vast majority of poly[*n*]rotaxanes studied to date are homocircuit[12] structures, at least in part because many are synthesized using solvophobic threading which, although synthetically efficient,[3] does not lend itself to the synthesis of heterocircuit targets.[13−15] Solvophobic threading can also lead to poor control of the threading ratio, a measure of the degree of axle encapsulation.[16] Conceptually, the simplest way to produce heterocircuit structures would be to design the axle with specific binding sites for each macrocycle. However, although poly[*n*]rotaxanes have been synthesized using such templating interactions,[17] this approach is synthetically more challenging and has not yet been applied in the synthesis of heterocircuit systems. Thus, although the effect on poly[*n*]-rotaxane properties of both the threading ratio, which could be considered the mechanical analogue of the degree of polymerization, and macrocycle structure, the mechanical equivalent of monomer structure, have been investigated,[3] to date little attention has been paid to the effect of the *order* of macrocycles in heterocircuit poly[*n*]rotaxanes, the mechanical analogue of monomer order in covalent polymers, currently a significant focus of research.[18]

Taking inspiration from the synthesis of information rich oligo-amides and oligo-nucleotides,[19] one approach to gain complete control over structure in a main-chain poly[*n*]-rotaxane is the use of iterative coupling strategies to sequentially add macrocycles to the growing axle.[20] Here we report the realization of such an iterative coupling methodology for the synthesis of oligo[*n*]rotaxanes with complete control over the order of macrocycles and excellent yield (>89%) for each cycle of mechanical bond formation. We demonstrate the power of our approach through the synthesis of a homo[6]-rotaxane and a hetero[4]rotaxane in excellent isolated yields.

RESULTS AND DISCUSSSION

Iterative Cu-mediated alkyne−azide cycloaddition (CuAAC) reactions[21] are an effective method for the synthesis of complex targets,[22,23] including sequence-controlled oligomers,[24] using a variety of methodologies[25,26] due to the efficiency of the triazole-forming step. The active template CuAAC (AT-CuAAC) reaction, introduced by Leigh and co-workers,[27] and modified by us to employ small macrocycles,[28] is a similarly efficient method for the synthesis of interlocked structures.[29,30] However, although the AT-CuAAC reaction often results in exceptionally high yields of interlocked molecules, reaction times often exceed 18 h and can be as long as 72 h for complete conversion, which is sub-optimal for iterative synthesis.

Optimization of the AT-CuAAC Reaction for Iterative Couplings. In order to optimize the conditions to shorten the reaction time, while maintaining the reaction yield, we first investigated the AT-CuAAC reaction of simple bis-alkyne **1**. This also allowed us to assess whether the second AT-CuAAC

Received: August 26, 2016
Published: October 4, 2016

DOI: 10.1021/jacs.6b08958
J. Am. Chem. Soc. 2016, 138, 16329−16336

reaction would proceed when the alkyne component was contained in an interlocked starting material, not a foregone conclusion by any means, and whether the presence of the second macrocyclic ligand would interfere with the Cu-mediated bond formation. When the reaction between bis-alkyne **1**, azide **2**, and macrocycle **3** was carried out in EtOH with N^{i}Pr$_2$Et as a base, consumption of **3** was found to be complete in 2 h at 100 °C under microwave (μw) irradiation (Scheme 1).[31] We initially anticipated that a mixture of

Scheme 1. Iterative Synthesis of [3]Rotaxane 6[a]

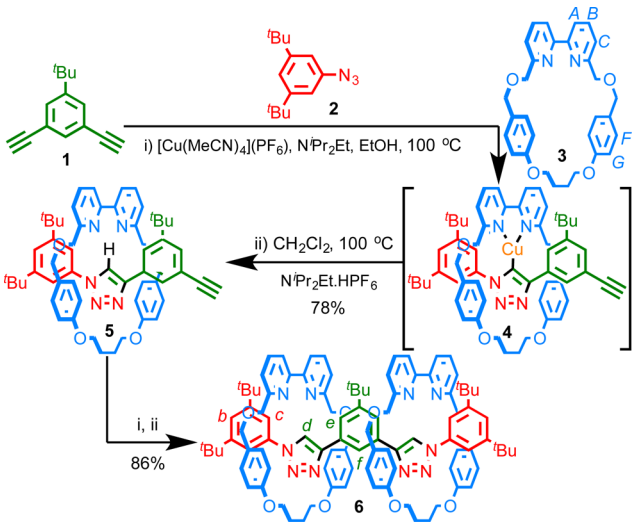

[a]Reagents and conditions: (i) 1 equiv each of **1**, **2**, **3**, and [Cu(MeCN)$_4$]PF$_6$, EtOH, 100 °C (μw), 2 h; (ii) CH_2Cl_2, 100 °C (μw), 1 h.

[2]rotaxane **5** and [3]rotaxane **6** would be formed, in keeping with the outcome of the corresponding reaction in the absence of the macrocycle **3**, which produces a statistical mixture of diyne **1** and mono- and bis-triazole products. However, ^{1}H NMR analysis of the product mixture after aqueous workup revealed two major products, [2]rotaxane **5** and a second, singly interlocked product which was tentatively identified as interlocked Cu triazolide **4**.[28b] Repeating the same reaction at room temperature gave **4** as the sole interlocked product and allowed it to be identified unambiguously by ^{1}H NMR (Figure 2b) and mass spectrometry (m/z = 958).

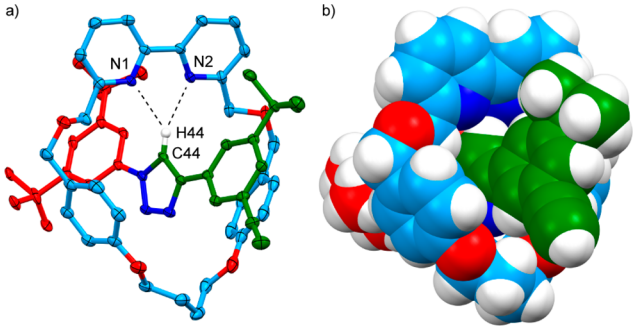

Figure 1. Solid-state structure of [2]rotaxane **5** in (a) ellipsoid and (b) space-filling representations. Interaction lengths (Å) and angles (deg): H44···N1 2.524, H44···N2 2.520, C44−H44···N1 138.5, C44−H44···N2 154.8.

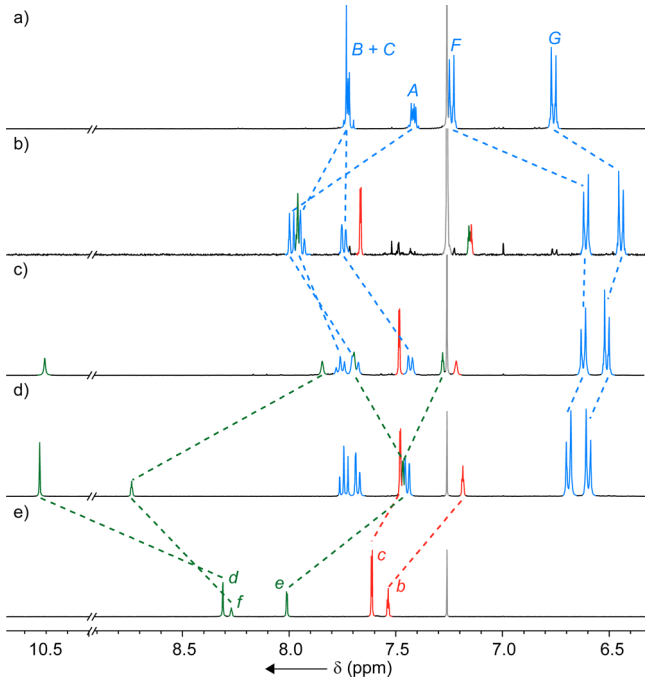

Figure 2. Partial ^{1}H NMR (400 MHz, $CDCl_3$, 298 K) with selected signals assigned of (a) macrocycle **3**, (b) crude reaction mixture containing triazolide **4** as the major product (>95%), (c) [2]rotaxane **5**, (d) [3]rotaxane **6**, and (e) corresponding non-interlocked axle of [3]rotaxane **6**. For macrocycle and axle labeling, see Scheme 1 (axle labeling as in **6**).

The high selectivity observed in the production of **5** is intriguing but potentially problematic, as the same steric shielding of the acetylene moiety could lead to poor efficiency or the need for longer reaction times in the second round of AT-CuAAC. Indeed, initial attempts to couple **5** with azide **2** and macrocycle **3** under the same AT-CuAAC conditions with sufficient Cu^I to coordinate to macrocycle **3** and [2]rotaxane **5** produced a poor yield of [3]rotaxane **6**, with the balance of material made up by the reaction of azide **2** and alkyne **5** to give the bis-triazole axle encircled by a single macrocycle. Working from the hypothesis that the steric hindrance of **5** might be exacerbated by the re-coordination of Cu^I into the macrocycle cavity, we repeated the AT-CuAAC reaction without additional Cu^I over and above that required to coordinate with macrocycle **3**. Pleasingly, under these conditions, the second mechanical bond formed efficiently, and after reprotonation of the corresponding triazolide byproduct by heating in CH_2Cl_2, [3]rotaxane **6** was isolated in 86% yield. Thus, under our optimized conditions over two steps, 2 equiv of azide **2** and macrocycle **3** were combined with bis-alkyne **1** to produce a doubly interlocked [3]rotaxane in 67% yield.

Analysis of [3]Rotaxane 6. Triazolide **4**, [2]rotaxane **5**, and [3]rotaxane **6** all display characteristic shifts in their ^{1}H NMR spectra (Figure 2b−d) consistent with their interlocked structure. In particular, as with all rotaxanes derived from **3**,[28a] protons H$_F$ and H$_G$ of the macrocycle (Figure 2a) appear at lower ppm than the non-interlocked macrocycle, and the triazole C−H signals in **5** and **6** resonate at higher ppm ($\Delta\delta$ = 2.33 and 2.22 ppm, respectively) than the non-interlocked axle, consistent with the presence of a C−H···N hydrogen bond, as observed in the solid-state structure of **5**.

Formation of the second mechanical bond to produce **6** increases the symmetry of the molecule, resulting in fewer

DOI: 10.1021/jacs.6b08958
J. Am. Chem. Soc. 2016, 138, 16329−16336

signals for the axle component compared with **5**. More unexpectedly, proton H_f of the axle resonates 0.46 ppm higher in [3]rotaxane **6** than in the non-interlocked axle (Figure 2e), and protons H_e resonate 0.56 ppm lower. This is surprising, considering the absence of similar effects or obvious non-covalent interactions between the macrocycle and equivalent protons in the solid-state structure of [2]rotaxane **5** (Figure 1). Computational modeling[32] of the non-interlocked axle suggested that the shielding of H_e and the deshielding of H_f may both be the result of conformational changes enforced by the sterically crowded mechanical bond; the predicted chemical shifts of protons H_e and H_f vary considerably, depending on the relative orientation of the central benzene ring and the triazole moieties.

Previous reports[23e,h] and molecular modeling[32] suggest that the non-interlocked axle adopts a range of conformations about the central benzene ring in which the *syn-syn* conformer is disfavored.[33] Conversely, the observed shielding of H_e and deshielding of H_f in [3]rotaxane **6** compared with the non-interlocked axle is consistent with the *syn-syn* rotamer being favored in the case of the [3]rotaxane. In keeping with this proposal, NOESY NMR analysis of **6** reveals strong cross-peaks between H_d and H_e but only a weak correlation between H_d and H_f (see Supporting Information). Models of **6** (Figure 3)

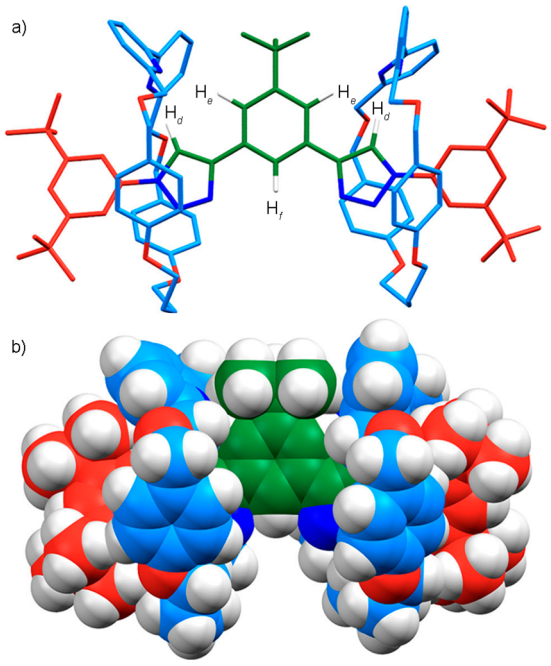

Figure 3. Computer model (PM6) of the proposed preferred *syn-syn* rotamer of [3]rotaxane **6** in (a) sticks and (b) space-filling representations.

indicate that steric interactions between the macrocycles are minimized in this conformation.[32] Thus, based on NMR analysis and molecular modeling, it appears that the sterically crowded nature of the mechanical bond stabilizes the *syn-syn* rotamer of [3]rotaxane **6**, leading to an unusual extended conformation in solution.

Iterative AT-CuAAC Synthesis of a Homo[6]rotaxane. In order to apply the conditions developed above to the iterative synthesis of oligomeric [*n*]rotaxanes, we synthesized building block **8** that incorporates an azide and a protected acetylene moiety.[25b,d] When alkyne **7** and azide **8** were subjected to our optimized AT-CuAAC conditions, macrocycle **3** was quantitatively converted into a mixture of [2]rotaxane **9** and the corresponding Cu^I triazolide (Scheme 2). Heating the crude AT-CuAAC product in CH_2Cl_2 led to protonolysis of the Cu−C bond. Subsequent TBAF-mediated proto-desilylation of the acetylene moiety produced [2]rotaxane **9**, which was isolated in 94% yield over three steps in one pot, requiring a total of 4 h reaction time. Repeating this sequence iteratively gave, in order, [3]rotaxane **10** (94%), [4]rotaxane **11** (91%), [5]rotaxane **12** (90%), and finally [6]rotaxane **13** (92%) without any significant loss of reaction efficiency. The yield of the final product was 67% over 15 steps with five rounds of purification to form five new mechanical bonds.

^{1}H NMR analysis confirmed the homogeneity of the isolated oligomeric products (Figure 4). As in rotaxanes **5** and **6**, triazole proton H_d of [2]rotaxane **9** resonates at >10 ppm (Figure 4a), suggesting that hydrogen-bonding interactions with the bipyridine of the macrocycle, as observed in the solid-state structure of **5** (Figure 1), are also present in **9**. Similarly, protons H_F and H_G of the flanking aromatic moieties are shifted to lower ppm in the interlocked structure. Introduction of the second macrocycle to give [3]rotaxane **10** (Figure 4b) leads to the appearance of a second distinct triazole signal at high ppm and another set of flanking aromatic protons between 6.6 and 6.9 ppm. Formation of the second mechanical bond leads to a triplet at 8.7 ppm, which is assigned as proton H_g of the axle. Subsequent iterations lead to distinct signals for the triazole, flanking aromatic rings of the macrocycle and the *ortho* proton of the linking benzene ring up until [6]rotaxane **13** (Figure 4e), where some signals become isochronous, indicating a transition from discrete proton environments to more oligomeric-type behavior.

The high chemical shifts of protons H_g, H_l, H_q, and H_v suggest that, as in [3]rotaxane **6**, [6]rotaxane **13** adopts a preferred conformation where the triazole rings are oriented with their N-atoms *syn*-periplanar to the central *ortho* proton of the linking aromatic units. ROESY NMR analysis of **13** is consistent with this proposal; weak correlations were observed between the central aromatic CH and the neighboring triazole protons, and strong correlations with the other C−H residues of the linking aromatic rings. Inspection of molecular models[32] once again suggests that this arrangement minimizes steric interactions between adjacent macrocycles. This leads to an extended conformation of the axle component and an end-to-end distance of ∼3.8 nm. In contrast, previously reported *meta*-linked phenyl-triazole oligomers are reported to adopt either helical conformations to maximize H-bonding and $\pi-\pi$ stacking,[23f,h] or alternating *syn-anti* conformations[23e,h] to minimize dipole−dipole interactions between adjacent polarized triazole moieties.

Iterative Synthesis of a Hetero[4]rotaxane. Having demonstrated the iterative AT-CuAAC synthesis of homo[*n*]-rotaxanes, we turned our attention to the synthesis of a heterocircuit analogue with precise control over the order of the different macrocycles. Reaction of macrocycle **14** with alkyne **7** and azide **8** (Scheme 3) resulted in quantitative conversion to the corresponding triazolide. In this case, heating the crude reaction product in CH_2Cl_2 did not lead to protonation of the Cu−C bond, presumably due to the more hindered environment provided by macrocycle **14**. As macrocycle **14** is stable to acidic conditions, TFA was employed to effect the required proto-demetalation. Subsequent proto-

DOI: 10.1021/jacs.6b08958
J. Am. Chem. Soc. 2016, 138, 16329−16336

Scheme 2. Iterative AT-CuAAC Synthesis of Oligo[*n*]rotaxanes[a]

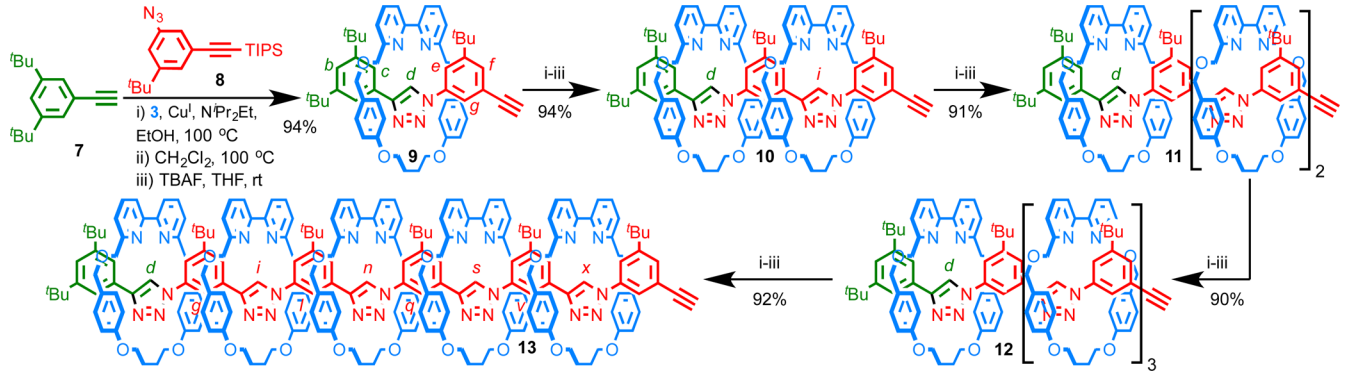

[a]Reagents and conditions: (i) 1 equiv each of **1**, **2**, **3**, and $[Cu(MeCN)_4]PF_6$, EtOH, 100 °C (μw), 2 h; (ii) CH_2Cl_2, 100 °C (μw), 1 h; (iii) TBAF, THF, rt, 1 h.

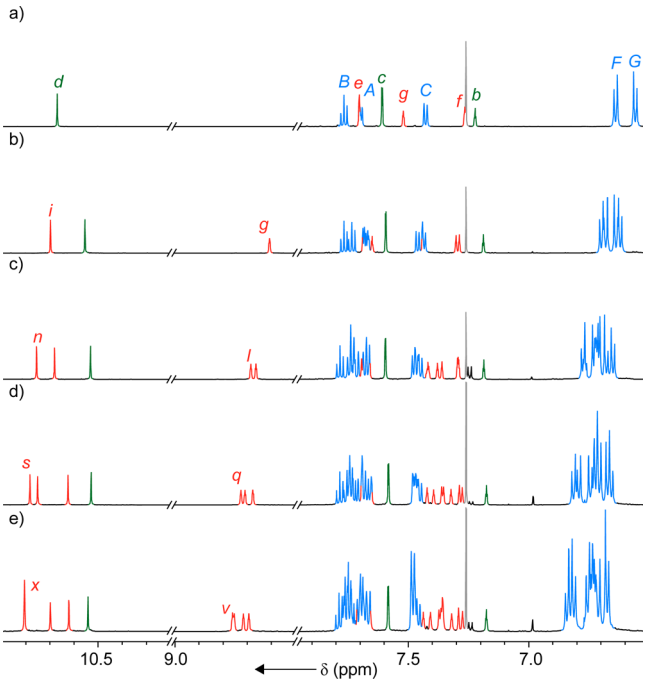

Figure 4. Partial ^{1}H NMR (500 MHz, $CDCl_3$, 298 K), with selected signals assigned,[34] of (a) [2]rotaxane **9**, (b) [3]rotaxane **10**, (c) [4]rotaxane **11**, (d) [5]rotaxane **12**, and (e) [6]rotaxane **13**. For macrocycle and axle labeling, see Schemes 1 and 2, respectively.

Scheme 3. Synthesis of Hetero[4]rotaxane 18[a]

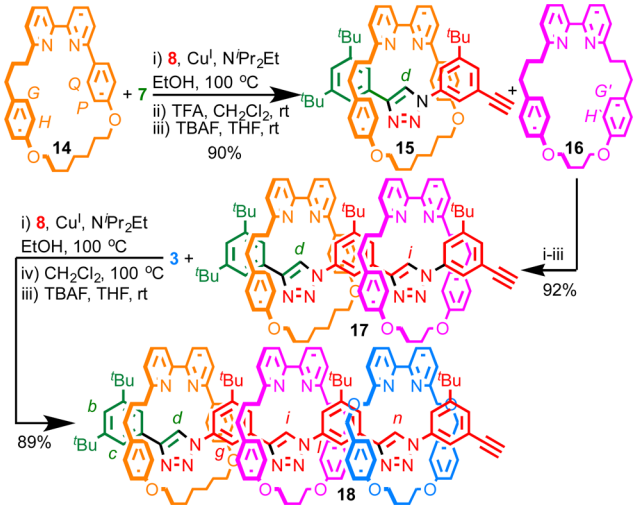

[a]Reagents and conditions: (i) 1 equiv each of **1**, **2**, **3**, and $[Cu(MeCN)_4]PF_6$, EtOH, 100 °C (μw), 2 h; (ii) TFA, CH_2Cl_2, rt, 1 h; (iii) TBAF, THF, rt, 1 h; (iv) CH_2Cl_2, 100 °C (μw), 1 h.

desilylation of the crude product with TBAF gave target [2]rotaxane **15** in 90% isolated yield over three chemical steps.

The lack of rotational symmetry in macrocycle **14** results in a more complicated ^{1}H NMR spectrum for [2]rotaxane **15** (Figure 5b) than those of [2]rotaxanes **5** and **9**, although the broad features (low-field triazole proton H_d, shielded flanking aromatic protons H_G, H_H, H_P, and H_Q) remain the same. Also, it is noteworthy that, as macrocycle **14** is rotationally unsymmetrical and the thread is translationally unsymmetrical, [2]rotaxane **15** is mechanically planar chiral,[28c] albeit formed as a racemic mixture. Indeed, single-crystal X-ray analysis (Figure 6) revealed that the unit cell contains both enantiomers of **15**, related by a center of inversion.

As the axle of [2]rotaxane **15** lacks prochiral units, which would be rendered diastereotopic in the interlocked structure, the chirality of **15** is not apparent in the ^{1}H NMR spectrum. However, it makes itself known when the second macrocycle is introduced. Using the same reaction sequence, [2]rotaxane **15** was converted into [3]rotaxane **17** by reaction with macrocycle **16** and azide **8** in excellent 92% yield. Despite being bilaterally symmetric, in [3]rotaxane **17** the mirror symmetry of macrocycle **16** is broken by the element of mechanical stereochemistry, and thus protons which are equivalent in the non-interlocked precursor are now diastereotopic and, in principle, may appear as non-equivalent in the ^{1}H NMR. This is most clearly demonstrated in the case of protons $H_{G'}$ and $H_{H'}$ of the flanking aromatic units, which appear as two sets of two coupled doublets, and protons $H_{C'}$, which appear as two overlapping doublets.

Similar effects are observed in [4]rotaxane **18**, which was produced in an excellent 89% yield by reaction of [3]rotaxane **17** with macrocycle **3** and azide **8**. ^{1}H NMR analysis of [4]rotaxane **18** (Figure 5d) revealed that not only are many of the resonances of macrocycle **16** non-equivalent, even signals arising from macrocycle **3** show evidence of desymmetrization by the element of mechanical chirality, with protons $H_{F''}$ and $H_{G''}$ appearing as complex multiplets. Although chiral information transfer over long distances in covalently bonded systems, typically through conformational biasing,[35] has

DOI: 10.1021/jacs.6b08958
J. Am. Chem. Soc. 2016, 138, 16329−16336

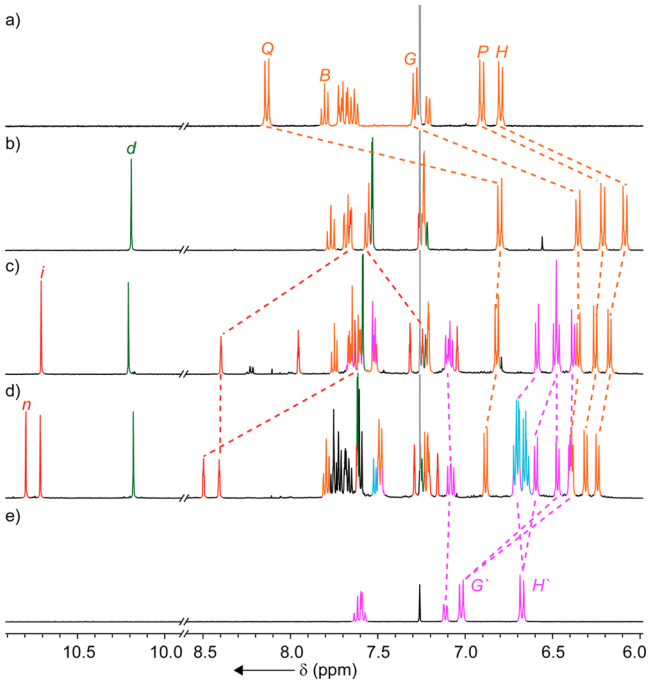

Figure 5. Partial ^{1}H NMR (500 MHz, $CDCl_3$, 298 K), with selected signals assigned,[34] of (a) macrocycle **14**, (b) [2]rotaxane **15**, (c) [3]rotaxane **17**, (d) [4]rotaxane **18**, and (e) macrocycle **16**. For labeling, see Scheme 3.

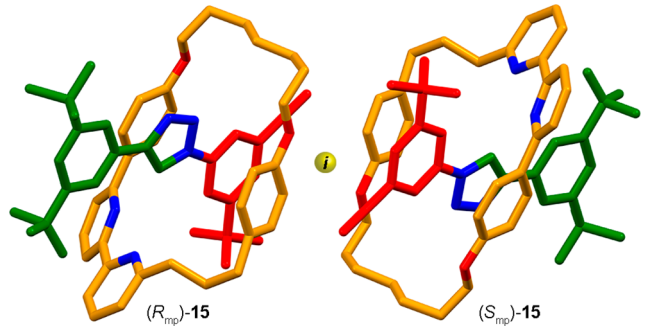

Figure 6. Solid-state structure of [2]rotaxane **15** showing both enantiomers of the mechanically chiral interlocked structures in the unit cell, related by the point of inversion (*i*).

previously been observed, the transfer of the mechanical stereochemical information centered on macrocycle **14** through the mechanical bond to macrocycle **16** is extremely unusual; in the case of [4]rotaxane **18**, molecular models[32] suggest a distance of 1.3 nm between the element of mechanical chirality and macrocycle **3**, assuming the axle adopts a *syn-syn* orientation, consistent with ROESY NMR analysis and the low-field shift of protons H_g and H_l.

CONCLUSIONS

In summary, we have successfully demonstrated an iterative AT-CuAAC approach for the high-yielding (~90% per mechanical bond) synthesis of both homo- and hetero[*n*]-rotaxanes. With regard to the latter, our iterative coupling approach allowed us to install three different macrocycles on the axle, with their order determined simply by the order in which the coupling reactions were carried out. Based on NMR analysis, supported by molecular modeling, the sterically crowded nature of the mechanical bond in the [*n*]rotaxane structures favors an unusual all-*syn* geometry of the axle component to minimize steric repulsion between the macrocycles, resulting in an extended conformation. With high-yielding and operationally convenient conditions in hand, it is now possible to synthesize oligo[*n*]rotaxanes rapidly with control over the structure of the axle (by varying the azide-acetylene monomer) and macrocycle. Furthermore, by electing to omit the macrocycle in some coupling steps, the threading ratio of the oligomeric product can be controlled precisely. Future work will focus on transferring the reaction to the solid phase to allow the automated synthesis of longer oligomers with precise control of their structure without the need for costly and time-consuming purification steps,[36] allowing designer oligo- and poly[*n*]rotaxanes to be investigated for a variety of applications.[37] Work toward this goal is currently taking place in our laboratory.

ASSOCIATED CONTENT

Supporting Information

The Supporting Information is available free of charge on the ACS Publications website at DOI: 10.1021/jacs.6b08958.

Full experimental details and characterization data for all novel compounds (PDF)
X-ray crystallographic data for [2]rotaxane **5** (CIF)
X-ray crystallographic data for [2]rotaxane **15** (CIF)
Pdb files for modeled structures 6, 13, 18, and S5 (ZIP)

AUTHOR INFORMATION

Corresponding Author

*s.goldup@soton.ac.uk

Author Contributions

§J.E.M.L. and J.W. contributed equally.

Notes

The authors declare no competing financial interest.
Processed NMR and other data supporting this study are openly available from the University of Southampton repository at http://doi.org/10.5258/SOTON/401444.

ACKNOWLEDGMENTS

The authors are grateful to Fluorochem for the gift of reagents. High-resolution mass spectrometry analysis was carried out by the EPSRC National Spectrometry Facility. This work was supported financially by the Royal Society, the European Union, and the EPSRC (EP/J01981X/1). This project has received funding from the European Union's Horizon 2020 research and innovation programme under the Marie Skłodowska-Curie grant agreement no. 660731. J.E.M.L. is an EU Marie Skłodowska-Curie Fellow. S.M.G. is a Royal Society Research Fellow.

REFERENCES

(1) Other classes of polyrotaxanes include side-chain, mechanically linked, and pseudorotaxane structures. For selected examples of these, see refs 4, 5, and 6, respectively.

(2) Although this is the most common class of main-chain poly[*n*]rotaxanes, alternative structures exist, such as polymers of macrocycles that are threaded by multiple axles.[3] For selected examples of multiply threaded discrete rotaxanes, see: (a) Klotz, E. J. F.; Claridge, T. D. W.; Anderson, H. L. *J. Am. Chem. Soc.* **2006**, *128*, 15374. (b) Prikhod'ko, A. I.; Sauvage, J.-P. *J. Am. Chem. Soc.* **2009**, *131*, 6794. (c) Cheng, H. M.; Leigh, D. A.; Maffei, F.; McGonigal, P. R.; Slawin, A. M. Z.; Wu, J. *J. Am. Chem. Soc.* **2011**, *133*, 12298. (d) Inouye, M.; Hayashi, K.; Yonenaga, Y.; Itou, T.; Fujimoto, K.; Uchida, T.; Iwamura, M.; Nozaki,

DOI: 10.1021/jacs.6b08958
J. Am. Chem. Soc. 2016, 138, 16329−16336

K. *Angew. Chem., Int. Ed.* **2014**, *53*, 14392. (e) Danon, J. J.; Leigh, D. A.; McGonigal, P. R.; Ward, J. W.; Wu, J. *J. Am. Chem. Soc.* **2016**, *138*, 12643.

(3) For selected reviews on polyrotaxanes and related structures, see: (a) Takata, T. *Polym. J.* **2006**, *38*, 1. (b) Araki, J.; Ito, K. *Soft Matter* **2007**, *3*, 1456. (c) Harada, A.; Hashidzume, A.; Yamaguchi, H.; Takashima, Y. *Chem. Rev.* **2009**, *109*, 5974. (d) Appel, E. A.; del Barrio, J.; Loh, X. J.; Scherman, O. A. *Chem. Soc. Rev.* **2012**, *41*, 6195. (e) Avestro, A.-J.; Belowich, M. E.; Stoddart, J. F. *Chem. Soc. Rev.* **2012**, *41*, 5881. (f) Arunachalam, M.; Gibson, H. W. *Prog. Polym. Sci.* **2014**, *39*, 1043. (g) Garcia-Rio, L.; Otero-Espinar, F.; Luzardo-Alvarez, A.; Blanco-Mendez, J. *Curr. Top. Med. Chem.* **2014**, *14*, 478. (h) Harada, A.; Takashima, Y.; Nakahata, M. *Acc. Chem. Res.* **2014**, *47*, 2128. (i) Wei, P.; Yan, X.; Huang, F. *Chem. Soc. Rev.* **2015**, *44*, 815.

(4) For selected examples of side-chain polyrotaxanes, see: (a) Born, M.; Ritter, H. *Angew. Chem., Int. Ed. Engl.* **1995**, *34*, 309. (b) Yu, G.; Suzaki, Y.; Abe, T.; Osakada, K. *Dalton Trans.* **2013**, *42*, 1476. (c) Suzuki, S.; Ishiwari, F.; Nakazono, K.; Takata, T. *Chem. Commun.* **2012**, *48*, 6478. (d) Bria, M.; Bigot, J.; Cooke, G.; Lyskawa, J.; Rabani, G.; Rotello, V. M.; Woisel, P. *Tetrahedron* **2009**, *65*, 400. (e) Sun, S.; Hu, X.-Y.; Chen, D.; Shi, J.; Dong, Y.; Lin, C.; Pan, Y.; Wang, L. *Polym. Chem.* **2013**, *4*, 2224.

(5) For selected examples of threaded supramolecular polymers and poly-pseudorotaxanes, see: (a) Mercer, D. J.; Vukotic, V. N.; Loeb, S. J. *Chem. Commun.* **2011**, *47*, 896. (b) Ogoshi, T.; Kayama, H.; Yamafuji, D.; Aoki, T.; Yamagishi, T. *Chem. Sci.* **2012**, *3*, 3221. (c) Ji, X.; Dong, S.; Wei, P.; Xia, D.; Huang, F. *Adv. Mater.* **2013**, *25*, 5725. (d) Li, C.; Han, K.; Li, J.; Zhang, Y.; Chen, W.; Yu, Y.; Jia, X. *Chem. - Eur. J.* **2013**, *19*, 11892. (e) Massoudi, A.; Adeli, M.; Khosravi far, L. *Int. J. Polym. Sci.* **2014**, *2014*, 1. (f) Huang, Z.; Yang, L.; Liu, Y.; Wang, Z.; Scherman, O. A.; Zhang, X. *Angew. Chem., Int. Ed.* **2014**, *53*, 5351. (g) Noor, A.; Moratti, S. C.; Crowley, J. D. *Chem. Sci.* **2014**, *5*, 4283. (h) Wei, P.; Yan, X.; Cook, T. R.; Ji, X.; Stang, P. J.; Huang, F. *ACS Macro Lett.* **2016**, *5*, 671. (i) Chen, D.; Zhan, J.; Zhang, M.; Zhang, J.; Tao, J.; Tang, D.; Shen, A.; Qiu, H.; Yin, S. *Polym. Chem.* **2015**, *6*, 25. (j) Gao, L.; Zheng, B.; Chen, W.; Schalley, C. A. *Chem. Commun.* **2015**, *51*, 14901. (k) Shi, Y.; Yang, Z.; Liu, H.; Li, Z.; Tian, Y.; Wang, F. *ACS Macro Lett.* **2015**, *4*, 6. (l) Zhang, W.; Zhang, H.-Y.; Zhang, Y.-H.; Liu, Y. *Chem. Commun.* **2015**, *51*, 16127.

(6) For selected examples of mechanically linked polymeric structures, see: (a) Li, S.; Zheng, B.; Chen, J.; Dong, S.; Ma, Z.; Huang, F.; Gibson, H. W. *J. Polym. Sci., Part A: Polym. Chem.* **2010**, *48*, 4067. (b) Hmadeh, M.; Fang, L.; Trabolsi, A.; Elhabiri, M.; Albrecht-Gary, A.-M.; Stoddart, J. F. *J. Mater. Chem.* **2010**, *20*, 3422. (c) Wei, P.; Yan, X.; Huang, F. *Chem. Commun.* **2014**, *50*, 14105. (d) Aoki, D.; Uchida, S.; Takata, T. *ACS Macro Lett.* **2014**, *3*, 324. (e) Aoki, D.; Uchida, S.; Takata, T. *Angew. Chem., Int. Ed.* **2015**, *54*, 6770. (f) Cao, P.-F.; Mangadlao, J. D.; de Leon, A.; Su, Z.; Advincula, R. C. *Macromolecules* **2015**, *48*, 3825. (g) Shi, Y.; Yang, Z.; Liu, H.; Li, Z.; Tian, Y.; Wang, F. *ACS Macro Lett.* **2015**, *4*, 6. (h) Nisar Ahamed, B.; Duchêne, R.; Robeyns, K.; Fustin, C.-A. *Chem. Commun.* **2016**, *52*, 2149.

(7) For selected examples of main-chain poly[*n*]rotaxanes for biomedical applications, see: (a) Li, J.; Li, X.; Zhou, Z.; Ni, X.; Leong, K. W. *Macromolecules* **2001**, *34*, 7236. (b) Li, J. *J. Drug Delivery Sci. Technol.* **2010**, *20*, 399. (c) Li, J. J.; Zhao, F.; Li, J. *Appl. Microbiol. Biotechnol.* **2011**, *90*, 427. (d) Yu, S.; Zhang, Y.; Wang, X.; Zhen, X.; Zhang, Z.; Wu, W.; Jiang, X. *Angew. Chem., Int. Ed.* **2013**, *52*, 7272. (e) Loh, X. J. *Mater. Horiz.* **2014**, *1*, 185. (f) Tamura, A.; Yui, N. *J. Biol. Chem.* **2015**, *290*, 9442.

(8) For selected examples of rotaxane-insulated molecular wires, see: (a) Taylor, P.; O'Connell, M.; McNeill, L.; Hall, M.; Aplin, R.; Anderson, H. *Angew. Chem., Int. Ed.* **2000**, *39*, 3456. (b) Brovelli, S.; Latini, G.; Frampton, M. J.; McDonnell, S. O.; Oddy, F. E.; Fenwick, O.; Anderson, H. L.; Cacialli, F. *Nano Lett.* **2008**, *8*, 4546. (c) Frampton, M. J.; Sforazzini, G.; Brovelli, S.; Latini, G.; Townsend, E.; Williams, C. C.; Charas, A.; Zalewski, L.; Kaka, N. S.; Sirish, M.; Parrott, L. J.; Wilson, J. S.; Cacialli, F.; Anderson, H. L. *Adv. Funct. Mater.* **2008**, *18*, 3367. (d) Mróz, M. M.; Lanzani, G.; Virgili, T.; Mc Donnell, S. O.; Frampton, M. J.; Anderson, H. L. *Phys. Rev. B: Condens. Matter Mater. Phys.* **2009**, *80*, 045111. (e) Terao, J.; Tsuda, S.; Tanaka, Y.; Okoshi, K.; Fujihara, T.; Tsuji, Y.; Kambe, N. *J. Am. Chem. Soc.* **2009**, *131*, 16004. (f) Oddy, F.; Brovelli, S.; Stone, M.; Klotz, E.; Cacialli, F.; Anderson, H. *J. Mater. Chem.* **2009**, *19*, 2846. (g) Brovelli, S.; Virgili, T.; Mroz, M. M.; Sforazzini, G.; Paleari, A.; Anderson, H. L.; Lanzani, G.; Cacialli, F. *Adv. Mater.* **2010**, *22*, 3690. (h) Masai, H.; Terao, J.; Tsuji, Y. *Tetrahedron Lett.* **2014**, *55*, 4035. (i) Masai, H.; Terao, J.; Makuta, S.; Tachibana, Y.; Fujihara, T.; Tsuji, Y. *J. Am. Chem. Soc.* **2014**, *136*, 14714.

(9) For examples of stimuli-responsive main-chain poly[*n*]rotaxanes, see: (a) Gibson, H. W.; Shen, Y. X.; Bheda, M. C.; Gong, C. *Polymer* **2014**, *55*, 3202. (b) Gong, C.; Gibson, H. *Angew. Chem., Int. Ed. Engl.* **1997**, *36*, 2331. (c) Fujita, H.; Ooya, T.; Yui, N. *Macromolecules* **1999**, *32*, 2534. (d) Ogoshi, T.; Nishida, Y.; Yamagishi, T.; Nakamoto, Y. *Macromolecules* **2010**, *43*, 7068.

(10) For selected examples of main-chain polyrotaxane-based sensors, see: (a) Zhu, S. S.; Carroll, P. J.; Swager, T. M. *J. Am. Chem. Soc.* **1996**, *118*, 8713. (b) Kwan, P. H.; MacLachlan, M. J.; Swager, T. M. *J. Am. Chem. Soc.* **2004**, *126*, 8638.

(11) For selected examples of slide-ring polymer gels, see: (a) Okumura, Y.; Ito, K. *Adv. Mater.* **2001**, *13*, 485. (b) Sakai, T.; Murayama, H.; Nagano, S.; Takeoka, Y.; Kidowaki, M.; Ito, K.; Seki, T. *Adv. Mater.* **2007**, *19*, 2023. (c) Ito, K. *Polym. J.* **2007**, *39*, 489. (d) Araki, J.; Ito, K. *Soft Matter* **2007**, *3*, 1456. (e) Kato, K.; Inoue, K.; Kidowaki, M.; Ito, K. *Macromolecules* **2009**, *42*, 7129. (f) Ito, K. *Curr. Opin. Solid State Mater. Sci.* **2010**, *14*, 28. (g) Kato, K.; Okabe, Y.; Okazumi, Y.; Ito, K. *Chem. Commun.* **2015**, *51*, 16180. (h) Kato, K.; Mizusawa, T.; Yokoyama, H.; Ito, K. *J. Phys. Chem. Lett.* **2015**, *6*, 4043.

(12) The terms "homocircuit" and "heterocircuit" have been used previously to describe catenanes and Borromean rings composed of constitutionally identical or different macrocycles, respectively; see ref 2c and the following: (a) Kidd, T. J.; Leigh, D. A.; Wilson, A. J. *J. Am. Chem. Soc.* **1999**, *121*, 1599. (b) Beves, J. E.; Blight, B. A.; Campbell, C. J.; Leigh, D. A.; McBurney, R. T. *Angew. Chem., Int. Ed.* **2011**, *50*, 9260. Here we apply these terms descriptively to distinguish between [*n*]rotaxanes composed of multiple identical macrocycles or two or more different macrocycles. In terms of nomenclature, these molecules are simply referred to as homo- and hetero[*n*]rotaxanes, respectively, and we use this convention when naming compounds.

(13) Solvophobic threading of macrocycles onto block copolymers has been shown to lead to block-selective recognition; for examples, see: (a) Li, J.; Ni, X.; Leong, K. *Angew. Chem., Int. Ed.* **2003**, *42*, 69. (b) Choi, H. S.; Ooya, T.; Sasaki, S.; Yui, N.; Ohya, Y.; Nakai, T.; Ouchi, T. *Macromolecules* **2003**, *36*, 9313. (c) Li, J.; Ni, X.; Zhou, Z.; Leong, K. W. *J. Am. Chem. Soc.* **2003**, *125*, 1788. (d) Chen, J.; Li, N.; Gao, Y.; Sun, F.; He, J.; Li, Y. *Soft Matter* **2015**, *11*, 7835. This would seem a logical approach to the synthesis of ordered polymeric hetero[*n*]rotaxanes. However, to our knowledge, this approach has not been realized to date.

(14) For an example of a random hetero[*n*]rotaxane produced by threading of two distinct α-CD derivatives onto a preformed polymeric axle, see: Tamura, M.; Gao, D.; Ueno, A. *J. Chem. Soc., Perkin Trans. 2* **2001**, 2012.

(15) For an example of polymeric hetero[*n*]rotaxanes containing β- and γ-CD, see: Herrmann, W.; Schneider, M.; Wenz, G. *Angew. Chem., Int. Ed. Engl.* **1997**, *36*, 2511.

(16) The exception to this is the "cooperative capture" approach to poly[*n*]rotaxanes: Hou, X.; Ke, C.; Stoddart, J. F. *Chem. Soc. Rev.* **2016**, *45*, 3766. This method combines solvophobic threading, cooperative interactions between cucurbit[6]uril (CB[6]) and β-cyclodextrin (β-CD), and an alkyne−azide cycloaddition reaction mediated by CB[6] to produce hetero[*n*]rotaxanes with 100% threading ratio and perfectly alternating β-CD and CB[6] macrocycles: Ke, C.; Smaldone, R. A.; Kikuchi, T.; Li, H.; Davis, A. P.; Stoddart, J. F. *Angew. Chem., Int. Ed.* **2013**, *52*, 381. For an example of the attempted synthesis of hetero[3]rotaxanes through similar complementary interactions between macrocycles, see: Wilson, E. A.; Vermeulen, N. A.; McGonigal, P.

DOI: 10.1021/jacs.6b08958
J. Am. Chem. Soc. 2016, 138, 16329−16336

R.; Avestro, A.-J.; Sarjeant, A. A.; Stern, C. L.; Stoddart, J. F. *Chem. Commun.* **2014**, *50*, 9665.
(17) For selected examples of main-chain poly[*n*]rotaxanes synthesized using specific templating interactions, see: (a) Zhang, W.; Dichtel, W. R.; Stieg, A. Z.; Benitez, D.; Gimzewski, J. K.; Heath, J. R.; Stoddart, J. F. *Proc. Natl. Acad. Sci. U. S. A.* **2008**, *105*, 6514. (b) Gibson, H. W.; Wang, H.; Niu, Z.; Slebodnick, C.; Zhakharov, L. N.; Rheingold, A. L. *Macromolecules* **2012**, *45*, 1270. (c) Belowich, M. E.; Valente, C.; Smaldone, R. A.; Friedman, D. C.; Thiel, J.; Cronin, L.; Stoddart, J. F. *J. Am. Chem. Soc.* **2012**, *134*, 5243. (d) Han, J. M.; Zhang, Y. H.; Wang, X. Y.; Liu, C. J.; Wang, J. Y.; Pei, J. *Chem. - Eur. J.* **2013**, *19*, 1502. (e) Kang, S.; Cetin, M. M.; Jiang, R.; Clevenger, E. S.; Mayer, M. F. *J. Am. Chem. Soc.* **2014**, *136*, 12588. (f) Nakazono, K.; Ishino, T.; Takashima, T.; Saeki, D.; Natsui, D.; Kihara, N.; Takata, T. *Chem. Commun.* **2014**, *50*, 15341.
(18) (a) Badi, N.; Lutz, J.-F. *Chem. Soc. Rev.* **2009**, *38*, 3383. (b) Lutz, J.-F.; Ouchi, M.; Liu, D. R.; Sawamoto, M. *Science* **2013**, *341*, 1238149.
(19) (a) Merrifield, R. B. *J. Am. Chem. Soc.* **1963**, *85*, 2149. (b) Beaucage, S. L.; Caruthers, M. H. *Tetrahedron Lett.* **1981**, *22*, 1859. (c) Caruthers, M. H. *Science* **1985**, *230*, 281. (d) Seeberger, P. H.; Haase, W.-C. *Chem. Rev.* **2000**, *100*, 4349. (e) Al Ouahabi, A.; Charles, L.; Lutz, J. F. *J. Am. Chem. Soc.* **2015**, *137*, 5629.
(20) For examples of iterative methods for the synthesis of interlocked molecules, see: (a) Daniell, H. W.; Klotz, E. J. F.; Odell, B.; Claridge, T. D. W.; Anderson, H. L. *Angew. Chem., Int. Ed.* **2007**, *46*, 6845. (b) Spruell, J. M.; Dichtel, W. R.; Heath, J. R.; Stoddart, J. F. *Chem. - Eur. J.* **2008**, *14*, 4168. (c) Fuller, A.-M. L.; Leigh, D. A.; Lusby, P. J. *J. Am. Chem. Soc.* **2010**, *132*, 4954. (d) Langton, M. J.; Matichak, J. D.; Thompson, A. L.; Anderson, H. L. *Chem. Sci.* **2011**, *2*, 1897. (e) Yamada, Y.; Okada, M.-A.; Tanaka, K. *Chem. Commun.* **2013**, *49*, 11053. (f) Heinrich, T.; Traulsen, C. H. H.; Holzweber, M.; Richter, S.; Kunz, V.; Kastner, S. K.; Krabbenborg, S. O.; Huskens, J.; Unger, W. E. S.; Schalley, C. A. *J. Am. Chem. Soc.* **2015**, *137*, 4382. (g) Wang, W.; Chen, L.-J.; Wang, X.-Q.; Sun, B.; Li, X.; Zhang, Y.; Shi, J.; Yu, Y.; Zhang, L.; Liu, M.; Yang, H.-B. *Proc. Natl. Acad. Sci. U. S. A.* **2015**, *112*, 5597. (h) Neal, E. A.; Goldup, S. M. *Angew. Chem., Int. Ed.* **2016**, *55*, 12488.
(21) (a) Rostovtsev, V. V.; Green, L. G.; Fokin, V. V.; Sharpless, K. B. *Angew. Chem., Int. Ed.* **2002**, *41*, 2596. (b) Tornøe, C. W.; Christensen, C.; Meldal, M. *J. Org. Chem.* **2002**, *67*, 3057.
(22) For recent reviews of the CuAAC reaction in multicomponent synthesis, see: (a) Meldal, M.; Tornøe, C. W. *Chem. Rev.* **2008**, *108*, 2952. (b) Johnson, J. A.; Finn, M. G.; Koberstein, J. T.; Turro, N. J. *Macromol. Rapid Commun.* **2008**, *29*, 1052. (c) Hassan, S.; Müller, T. J. J. *Adv. Synth. Catal.* **2015**, *357*, 617. (d) Castro, V.; Rodríguez, H.; Albericio, F. *ACS Comb. Sci.* **2016**, *18*, 1.
(23) For selected examples of the iterative CuAAC reaction in synthesis, see: (a) Angelo, N. G.; Arora, P. S. *J. Am. Chem. Soc.* **2005**, *127*, 17134. (b) Such, G. K.; Quinn, J. F.; Quinn, A.; Tjipto, E.; Caruso, F. *J. Am. Chem. Soc.* **2006**, *128*, 9318. (c) Vestberg, R.; Malkoch, M.; Kade, M.; Wu, P.; Fokin, V. V.; Barry Sharpless, K.; Drockenmuller, E.; Hawker, C. J. *J. Polym. Sci., Part A: Polym. Chem.* **2007**, *45*, 2835. (d) Li, Y.; Flood, A. H. *Angew. Chem., Int. Ed.* **2008**, *47*, 2649. (e) Juwarker, H.; Lenhardt, J. M.; Pham, D. M.; Craig, S. L. *Angew. Chem., Int. Ed.* **2008**, *47*, 3740. (f) Meudtner, R. M.; Hecht, S. *Angew. Chem., Int. Ed.* **2008**, *47*, 4926. (g) Luo, L.; Frisbie, C. D. *J. Am. Chem. Soc.* **2010**, *132*, 8854. (h) Hua, Y.; Ramabhadran, R. O.; Karty, J. A.; Raghavachari, K.; Flood, A. H. *Chem. Commun.* **2011**, *47*, 5979. (i) Ehlers, I.; Maity, P.; Aubé, J.; König, B. *Eur. J. Org. Chem.* **2011**, *2011*, 2474. (j) Ingale, S. A.; Seela, F. *J. Org. Chem.* **2013**, *78*, 3394. (k) Lewandowski, B.; De Bo, G.; Ward, J. W.; Papmeyer, M.; Kuschel, S.; Aldegunde, M. J.; Gramlich, P. M. E.; Heckmann, D.; Goldup, S. M.; D'Souza, D. M.; Fernandes, A. E.; Leigh, D. A. *Science* **2013**, *339*, 189. (l) Galibert, M.; Piller, V.; Piller, F.; Aucagne, V.; Delmas, A. F. *Chem. Sci.* **2015**, *6*, 3617. (m) Shang, J.; Zhao, W.; Li, X.; Wang, Y.; Jiang, H. *Chem. Commun.* **2016**, *52*, 4505. (n) Zurro, M.; Asmus, S.; Bamberger, J.; Beckendorf, S.; García Mancheño, O. *Chem. - Eur. J.* **2016**, *22*, 3785.
(24) For examples of iterative synthesis of triazole oligomers, see: (a) Barnes, J. C.; Ehrlich, D. J. C.; Gao, A. X.; Leibfarth, F. A.; Jiang, Y.; Zhou, E.; Jamison, T. F.; Johnson, J. A. *Nat. Chem.* **2015**, *7*, 810. (b) Jiang, Y.; Golder, M. R.; Nguyen, H. V.-T.; Wang, Y.; Zhong, M.; Barnes, J. C.; Ehrlich, D. J. C.; Johnson, J. A. *J. Am. Chem. Soc.* **2016**, *138*, 9369.
(25) For examples of iterative CuAAC methodologies, see: (a) Lu, G.; Lam, S.; Burgess, K. *Chem. Commun.* **2006**, 1652. (b) Aucagne, V.; Leigh, D. A. *Org. Lett.* **2006**, *8*, 4505. (c) Kaliappan, K. P.; Kalanidhi, P.; Mahapatra, S. *Synlett* **2009**, *2009*, 2162. (d) Valverde, I. E.; Delmas, A. F.; Aucagne, V. *Tetrahedron* **2009**, *65*, 7597. (e) Stefani, H. A.; Canduzini, H. A.; Manarin, F. *Tetrahedron Lett.* **2011**, *52*, 6086. (f) Aizpurua, J. M.; Sagartzazu-Aizpurua, M.; Azcune, I.; Miranda, J. I.; Monasterio, Z.; García-Lecina, E.; Fratila, R. M. *Synthesis* **2011**, *2011*, 2737. (g) Yuan, Z.; Kuang, G.-C.; Clark, R. J.; Zhu, L. *Org. Lett.* **2012**, *14*, 2590. (h) Ingale, S. A.; Seela, F. *J. Org. Chem.* **2013**, *78*, 3394. (i) Pancholi, J.; Hodson, D. J.; Jobe, K.; Rutter, G. A.; Goldup, S. M.; Watkinson, M. *Chem. Sci.* **2014**, *5*, 3528. (j) Hatit, M. Z. C.; Sadler, J. C.; McLean, L. A.; Whitehurst, B. C.; Seath, C. P.; Humphreys, L. D.; Young, R. J.; Watson, A. J. B.; Burley, G. A. *Org. Lett.* **2016**, *18*, 1694.
(26) For an alternative methodology that combines iterative amide bond formation with the CuAAC reaction, see: Holub, J. M.; Jang, H.; Kirshenbaum, K. *Org. Biomol. Chem.* **2006**, *4*, 1497.
(27) (a) Aucagne, V.; Hänni, K. D.; Leigh, D. A.; Lusby, P. J.; Walker, D. B. *J. Am. Chem. Soc.* **2006**, *128*, 2186. (b) Aucagne, V.; Berna, J.; Crowley, J. D.; Goldup, S. M.; Hänni, K. D.; Leigh, D. A.; Lusby, P. J.; Ronaldson, V. E.; Slawin, A. M. Z.; Viterisi, A.; Walker, D. B. *J. Am. Chem. Soc.* **2007**, *129*, 11950.
(28) (a) Lahlali, H.; Jobe, K.; Watkinson, M.; Goldup, S. M. *Angew. Chem., Int. Ed.* **2011**, *50*, 4151. (b) Winn, J.; Pinczewska, A.; Goldup, S. M. *J. Am. Chem. Soc.* **2013**, *135*, 13318. (c) Bordoli, R. J.; Goldup, S. M. *J. Am. Chem. Soc.* **2014**, *136*, 4817. (d) Neal, E. A.; Goldup, S. M. *Chem. Sci.* **2015**, *6*, 2398. (e) Galli, M.; Lewis, J. E. M.; Goldup, S. M. *Angew. Chem., Int. Ed.* **2015**, *54*, 13545. (f) Lewis, J. E. M.; Bordoli, R. J.; Denis, M.; Fletcher, C. J.; Galli, M.; Neal, E. A.; Rochette, E. M.; Goldup, S. M. *Chem. Sci.* **2016**, *7*, 3154.
(29) For a review of the active template approach more generally, see: Crowley, J. D.; Goldup, S. M.; Lee, A.-L.; Leigh, D. A.; McBurney, R. T. *Chem. Soc. Rev.* **2009**, *38*, 1530.
(30) Other metal-mediated bond formations have been adapted for the active template synthesis of interlocked molecules. For selected examples, see: (a) Saito, S.; Takahashi, E.; Nakazono, K. *Org. Lett.* **2006**, *8*, 5133. (b) Berná, J.; Crowley, J. D.; Goldup, S. M.; Hänni, K. D.; Lee, A.-L.; Leigh, D. A. *Angew. Chem., Int. Ed.* **2007**, *46*, 5709. (c) Crowley, J. D.; Hänni, K. D.; Lee, A.; Leigh, D. A. *J. Am. Chem. Soc.* **2007**, *129*, 12092. (d) Berná, J.; Goldup, S. M.; Lee, A.-L.; Leigh, D. A.; Symes, M. D.; Teobaldi, G.; Zerbetto, F. *Angew. Chem., Int. Ed.* **2008**, *47*, 4392. (e) Crowley, J. D.; Goldup, S. M.; Gowans, N. D.; Leigh, D. A.; Ronaldson, V. E.; Slawin, A. M. Z. *J. Am. Chem. Soc.* **2010**, *132*, 6243. (f) Crowley, J. D.; Hänni, K. D.; Leigh, D. A.; Slawin, A. M. Z. *J. Am. Chem. Soc.* **2010**, *132*, 5309. (g) Crowley, J. D.; Goldup, S. M.; Gowans, N. D.; Leigh, D. A.; Ronaldson, V. E.; Slawin, A. M. Z. *J. Am. Chem. Soc.* **2010**, *132*, 6243. (h) Ugajin, K.; Takahashi, E.; Yamasaki, R.; Mutoh, Y.; Kasama, T.; Saito, S. *Org. Lett.* **2013**, *15*, 2684. (i) Cheng, H. M.; Leigh, D. A.; Maffei, F.; McGonigal, P. R.; Slawin, A. M. Z.; Wu, J. *J. Am. Chem. Soc.* **2011**, *133*, 12298. (j) Langton, M. J.; Xiong, Y.; Beer, P. D. *Chem. - Eur. J.* **2015**, *21*, 18910.
(31) Heating in an oil bath gave similar isolated yields of the target rotaxanes. However, microwave irradiation was more operationally convenient, as it ensures accurate heating and thus reproducible reaction times, as well as being more energy efficient.
(32) Modeling was carried out using Spartan '10 (Wavefunction Inc.). Rotaxanes **6** (*syn-syn*, *syn-anti*, and *anti-anti* conformations), **13**, and **18** were modeled using semiempirical methods (PM6). The non-interlocked axle of [3]rotaxane **6** was modeled using DFT (B3LYP, 6-31G*). For full details, see the Supporting Information.
(33) A small number of solid-state structures for *N,N′*-aryl *meta*-bis-triazole benzenes similar to the non-interlocked axle of **6** have been

DOI: 10.1021/jacs.6b08958
J. Am. Chem. Soc. 2016, 138, 16329−16336

reported, all but one of which (ref 33b) exhibit *syn-anti* or *anti-anti* conformations in the solid state. However, given that all examples feature close intermolecular contacts and, in many cases, H-bonding interactions with co-crystalized solvent, it is perhaps unwise to extrapolate from these solid-state structures to the solution-state conformations of these molecules: (a) García, F.; Torres, M. R.; Matesanz, E.; Sánchez, L. *Chem. Commun.* **2011**, *47*, 5016. (b) White, N. G.; Beer, P. D. *Supramol. Chem.* **2012**, *24*, 473. (c) Asmus, S.; Beckendorf, S.; Zurro, M.; Mück-Lichtenfeld, C.; Fröhlich, R.; García Mancheño, O. *Chem. - Asian J.* **2014**, *9*, 2178.

(34) Wherever possible, signals are colored according to the component from which they are derived, as in the relevant reaction scheme. However, in the case of complex multiplets derived from multiple components, the color coding is indicative only. See Supporting Information for detailed assignments of signals.

(35) Clayden, J. *Chem. Soc. Rev.* **2009**, *38*, 817.

(36) A reviewer suggested that, given the excellent yields achieved over each chain elongation sequence, it might be possible to carry out the reactions described above without purification between the deprotection and AT-CuAAC steps. Although this is extremely synthetically attractive, the presence of TBAF and other tetrabutylammonium salts that are incompletely removed during aqueous workup can interfere with the AT-CuAAC reaction. Furthermore, even minor quantities of "defective" chains, particularly in the case of heterocircuit structures, amplified over many rounds of AT-CuAAC reaction, would be extremely difficult to separate. Reactions on solid support solve both of these problems by allowing excess reagents to be used and removed at each step. An alternative suggestion was to do away with protecting groups altogether (which would circumvent some of the above issues) by relying on steric control in the reaction of diyne **1** and its diazide counterpart. Sadly, this is not possible in the current system; simple molecular models reveal that the azide functional group is not sufficiently bulky to prevent the macrocycle from escaping the axle in the AT-CuAAC products of these monomers. This is, however, an excellent alternative approach, and we are actively investigating how it could be achieved with different monomers.

(37) The CuAAC reaction has already been demonstrated to be an effective tool in solid-phase synthesis.[22,25b,26]

DOI: 10.1021/jacs.6b08958
J. Am. Chem. Soc. 2016, 138, 16329−16336